JOURNAL OF CATALYSIS **161,** 211–221 (1996)
ARTICLE NO. 0179

Selective Catalytic Reduction of NO with NH_3 over Supported Vanadia Catalysts

Israel E. Wachs,*[,1] Goutam Deo,* Bert M. Weckhuysen,*[,2] Amedeo Andreini,† Michael A. Vuurman,† Michiel de Boer,† and Michael D. Amiridis‡

*Zettlemoyer Center for Surface Studies, Department of Chemical Engineering, Lehigh University, Bethlehem, Pennsylvania 18015; †Department of Chemical Technology, University of Amsterdam, Nieuwe Achtergracht 166, 1018 WV, Amsterdam, The Netherlands; and ‡Department of Chemical Engineering, Swearingen Engineering Center, University of South Carolina, Columbia, South Carolina 29208

Received July 6, 1995; revised February 6, 1996; accepted February 13, 1996

The selective catalytic reduction (SCR) of NO with NH_3 was systematically investigated over a series of supported vanadia catalysts to obtain additional insight into this important industrial reaction. The influence of surface vanadia coverage, promoters (surface tungsten oxide, niobium oxide, and sulfate species), and the specific oxide support (TiO_2, Al_2O_3, and SiO_2) was examined. The molecular structures of the surface metal oxide species were determined by *in situ* Raman spectroscopy, and the corresponding surface acidity properties were monitored with infrared spectroscopy employing pyridine adsorption. The redox properties of the surface metal oxide species were probed with the sensitive methanol oxidation reaction and temperature-programmed reduction. The SCR reactivity of the various catalysts was determined over a wide temperature range. The current findings suggest that a dual-site (a surface vanadia redox site and an adjacent nonreducible metal oxide site) mechanism is required for the efficient selective catalytic reduction of NO with NH_3 over supported vanadia catalysts. The SCR reaction is sensitive to the immediate environment of the surface vanadia species: overall surface coverage of the metal oxide overlayer (factor of 5 in turnover frequency), nature of adjacent surface metal oxide species (factor of 10 in turnover frequency) and oxide support ligands (factor of 3 in turnover frequency). The SCR reaction, however, does not appear to depend on the specific structure of the surface vanadia species. The SCR selectivity toward N_2 formation also varies with the immediate environment of the surface vanadia species. The selectivity depends on the specific oxide support ($TiO_2 > Al_2O_3 > SiO_2$), temperature (decreases at higher temperature due to oxidation of NH_3 and NO to N_2O), and surface concentration of redox sites (decreases with the concentration of pairs of redox sites). The SCR reaction is not related to the properties of the terminal V=O bond since *in situ* Raman studies during SCR, employing $V=^{18}O$, demonstrate that this bond is relatively stable under reaction conditions (possessing a lifetime that is ~10 times the characteristic reaction time). Thus, the bridging V–O–support bond appears to be involved in the rate-determining step. © 1996 Academic Press, Inc.

INTRODUCTION

The selective catalytic reduction of NO_x with NH_3 over supported V_2O_5–WO_3/TiO_2 catalysts is an important commercial technology for the reduction of NO_x emissions from power plants. The industrial success of the selective catalytic reduction (SCR) reaction has generated many investigations, but many fundamental questions about the nature of the catalytic active site and mechanism of this reaction still remain.

Miyamoto *et al.* proposed that NH_3 is strongly adsorbed adjacent to V=O sites as NH_4^+ and that the reaction rate is directly proportional to the number of surface V=O bonds which were determined by a rectangular pulse technique (1). Janssen *et al.* employed oxygen isotope experiments to probe the surface vanadia species and proposed that a pyrovanadate structure, O=V–O–V=O, was the most likely structure for the active site (2). Went *et al.* characterized the surface vanadia species with *in situ* Raman spectroscopy as well as temperature-programmed reduction/temperature-programmed oxidation and concluded that both monomeric vanadyl and polymeric vanadate surface species were present on the titania support (3); corresponding SCR studies suggested that the polymeric species were about 10 times more active than the monomeric species, but the polymeric species were less selective toward N_2 formation (4). The increase in the SCR specific activity with surface vanadia coverage on titania has also been reported by other investigators (5, 6). Lietti *et al.* proposed that the redox properties of the catalyst are a major factor governing activity and that the reaction involved primarily a coordinated ammonia species on Lewis acid sites (6, 7). The potential participation of a protonated ammonium on a surface Brønsted acid site was also proposed because of the possible interconversion of these species (6, 7). Ramis *et al.* also proposed that promoters affect the Lewis acidity of V=O bonds which affects the adsorption of ammonia, the first step in the SCR reaction (8). Based on *in situ* FT-IR studies, Topsoe proposed that Brønsted

[1] To whom correspondence should be addressed.

[2] Current address: Centrum voor Oppervlaktechemie en Katalyse, K. U. Leuven, Kardinaal Mereierlaan 92, B-3001 Heverlee, Belgium.

0021-9517/96 $18.00
Copyright © 1996 by Academic Press, Inc.
All rights of reproduction in any form reserved.

acid sites are the main active sites for the SCR reaction over titania-supported vanadia catalysts (9). The role of Brønsted acidity in the SCR reaction over supported vanadia catalysts was also suggested by other research groups (10, 11). Model SCR studies with unsupported V_2O_5 crystals concluded that the crystallographic planes possessing V–O–V or V–OH bonds rather than V=O bonds were the selective sites for the SCR reaction (12, 13). In a recent series of detailed studies over vanadia–titania catalysts, Topsoe *et al.* combined *in situ* FT-IR and on-line mass spectrometry studies, transient as well as steady state, to provide convincing evidence that both surface Brønsted acid sites and surface V=O sites are involved in the SCR catalytic cycle (14, 15).

The mechanism of the selective catalytic reduction of NO with ammonia over vanadia–titania catalysts has been proposed to occur both by an Eley–Rideal mechanism (1, 2, 6, 7, 12, 15) and by a Langmuir–Hinshelwood mechanism (4, 16, 17). However, significant amounts of adsorbed NO are not found on the vanadia–titania catalyst surface under reaction conditions (15). Furthermore, detailed microkinetic analysis of the SCR reaction by Dumesic *et al.* suggests that a simple two-step Eley–Rideal mechanism involving reaction between adsorbed NH_3 and gaseous (or weakly adsorbed) NO is also not consistent with the data (18). The SCR kinetic data could quantitatively be described by a kinetic model involving a three-step mechanism: equilibrated ammonia adsorption, activation of adsorbed ammonia, and reaction between activated ammonia and NO (gaseous or weakly adsorbed). The surface sites associated with these three reaction steps have been proposed to involve surface Brønsted acid sites, surface V=O sites, and reduced surface V=O sites (15).

This investigation was initiated to obtain additional fundamental insights into the nature of the active sites of supported vanadia catalysts employed in the selective catalytic reduction of NO with NH_3. A major objective was to determine how the structure and reactivity of the surface vanadia species are influenced by surface coverage, promoters (surface tungsten oxide, niobium oxide, silica, and sulfate species), the specific oxide support (TiO_2, Al_2O_3, and SiO_2), and temperature. The dehydrated molecular structures of the surface metal oxide species were determined by Raman spectroscopy. The surface Brønsted and Lewis acidity were determined by IR experiments employing pyridine adsorption as a probe molecule. The redox potential of the surface metal oxide species was probed by the methanol oxidation reaction and temperature-programmed reduction (TPR). The DeNOx SCR reactivity of the catalysts was expressed as turnover frequencies (TOFs) to allow for a fundamental comparison between the molecular structure and the specific reactivity of the active sites present in these catalysts. The systematic variation of the parameters present in catalysts employed for the selective catalytic reduction of NO with NH_3 provided additional fundamental insights into the nature of the active sites present in SCR catalysts.

EXPERIMENTAL

Preparation of Supported Vanadium Oxide Catalysts

The oxide supports used for the preparation of supported vanadium oxide catalysts were TiO_2 (50 m^2/g, Degussa), Al_2O_3 (180 m^2/g, Harshaw), and SiO_2 (300 m^2/g, Cabot). The vanadium oxide precursor used for this study was vanadium triisopropoxide (Alfa, 95–98% purity), and the method used for the preparation was incipient wetness impregnation. The moisture- and air-sensitive nature of this precursor required that the prepation be performed in a nitrogen environment and using nonaqueous solvents. Known amounts of the precursor and methanol (Fisher-certified ACS, 99.9% pure), corresponding to incipient wetness impregnation volume and final amount of vanadium oxide required, were prepared in a glove box filled with nitrogen, mixed thoroughly with the oxide support, and let to stand for 16 h. This was followed by various heat treatments in nitrogen and the final calcination was performed at 723 K for all the supported vanadium oxide catalysts (19).

Preparation of Promoted 1% V_2O_5/TiO_2 Catalysts

The oxides of tungsten, niobium, and sulfur were added to 1% V_2O_5/TiO_2 to study the effect of the promoters on supported vanadium oxide catalysts. The precursors and solvent used for tungsten oxide, niobia, and sulfur oxide were ammonium metatungstate and water, niobium ethoxide (moisture and air sensitive) and propanol, and ammonium sulfate and water, respectively. Known amounts of precursor and solvent were thoroughly mixed with a previously prepared 1% V_2O_5/TiO_2 in a nitrogen-filled glove box (niobium ethoxide) or in the ambient (ammonium metatungstate and ammonium sulfate) and let to sit for 16 h (20, 21). The niobium oxide-promoted sample was then heated similar to vanadium oxide-supported samples. The tungsten oxide- and sulfur oxide-promoted samples were gradually heated in oxygen (or air) up to 723 K.

Raman Spectrometer

Laser Raman spectra were obtained with an Ar^+ laser (Spectra Physics, Model 165). The incident laser was tuned to 514.5 nm and delivered 50–100 mW of power measured at the sample. The scattered radiation from the sample was collected at right angles to the laser beam and directed into an OMA III (Princeton Applied Research, Model 1463 optical multichannel analyzer) with a photodiode array detector thermoelectrically cooled to 238 K. About 100–200 mg of the pure catalyst was made into a wafer and placed in the *in situ* cell. The *in situ* cell contained a rotating cell, thermocouple probe, and inlet and outlet gas connections.

The arrangment of the *in situ* cell has been outlined elsewhere (22). To obtain the Raman spectra under dehydration conditions the *in situ* cell was heated to 623 K for $\frac{1}{2}$ h to desorb the surface moisture and then cooled to room temperature to enhance the signal. The entire procedure was performed in a stream of flowing oxygen (Linde Speciality Grade, 99.99% purity). The Raman spectra of the catalysts were also obtained under ambient conditions and checked for the effect of hydration–dehydration and, consequently, compound formation. No compound formation was observed for any of the samples.

In situ Raman spectroscopy for the selective catalytic reduction of NO with NH_3 was performed at 300°C on a 4% V_2O_5/ZrO_2 sample. The fresh catalyst was dehydrated *in situ* in a O_2 stream (Linde Speciality Grade, 99.99% purity) at 500°C for $\frac{1}{2}$ h and then coooled to 450°C. The dehydrated sample was then reduced in a stream of C_4H_{10}/He gas mixture and reoxidized in a stream of $^{18}O_2$/He mixture (JWS Technologies, Inc., Matheson, $^{18}O_2$/He = 3/97) at 450°C. Repeating the reduction (in C_4H_{10}/He) and reoxidation (in $^{18}O_2$/He) at 450°C maximized the degree of oxygen-18 isotopic exchange. The selective catalytic reduction experiments were then performed *in situ* using a reaction mixture of 500 ppm NO, 500 ppm NH_3, 50,000 ppm $^{16}O_2$, and a balance of He. The entire dehydration–reduction–reoxidation–reaction procedure was performed *in situ* without ever exposing the sample to ambient conditions.

Methanol Oxidation Reaction

The methanol oxidation reaction was performed in a differential upflow reactor using a CH_3OH/O_2/He gas mixture in the molar ratio of ~6/13/81 and flowing at ~100 sccm. The products from the reactor were analyzed by a gas chromatograph (HP5840A) using two TCDs and a FID with two packed columns (Poropak R and Carbosieve SII) connected in parallel. The amount of catalyst was controlled to achieve less than 10% methanol conversion. The TOF for methanol oxidation was defined as molecules of methanol converted per molecule surface vanadium oxide site per second. Raman spectroscopy demonstrated that vanadium oxide was 100% dispersed below monolayer coverage (6% V_2O_5/TiO_2). Additional details regarding the methanol oxidation reaction setup can be found elsewhere (19).

DeNOx Reaction

The DeNOx reaction was carried out using a O_2 (2%), NO (500 ppm), NH_3 (550 ppm), and balance He (supplied by UCAR—Union Carbide) gas mixture. The gases were fed to a static gas mixing tube (MT) through four mass controllers (Hi-Tec MFC 201) to provide a total flow of 50 cm^3-/min. The gas mixing section was made up of stainless-steel tubing maintained at 383 K. The reactant gas mixture was divided into seven streams in a splitter: six streams, adjusted by six mass flow controllers, were admitted to the six reactors and the seventh stream, consisting of excess mixture, was vented through a backpressure controller (Tescom mod. 26-2321-24) to maintain a constant pressure in the system. The reactor section is made up of a water-cooled oven controlled by a temperature-programmed controller (West 2050) carrying six glass reactors (Duran 50) which could be simultaneously tested. Within the oven, the reactor tubes extended through a cylindrical aluminum block designed to ensure a uniform temperature profile. The temperature in the oven was measured by means of a chromel–alumel thermocouple. The temperature was not found to differ from that prevailing inside the reactors under the test conditions.

The analysis of the reactants and products were performed with a mass spectrometer interfaced with a IBM-PC/AT computer. An air-actuated multiposition valve (Valco SD type) selects one of the product streams for admission to the mass spectrometer. This took place by differential pumping through a capillary tube ($L = 1.10$ m, i.d. = 0.15 mm) and a small orifice. Calibration gas mixtures were used to quantify product concentrations. An internal standard technique was also applied to improve the accuracy of the measurements. The TOF for the SCR of NO_x with NH_3 was defined as the molecules of NO converted per surface vanadium oxide site per second. Raman spectroscopy demonstrated that vanadium oxide was 100% dispersed below monolayer coverages (6% V_2O_5/TiO_2). Additional details of the DeNOx reaction system can be found elsewhere (23).

Acidity Measurements

For the acidity measurements, pyridine was adsorbed at 423 K followed by an hour evacuation of the sample at approximately 773 K. A saturated pyridine-in-helium mixture was created by passing a helium stream through a pyridine container maintained at 273 K. The samples were exposed to this mixture for 2 h, and then evacuated at 453 K to remove the weakly held pyridine. The diffuse reflectance IR-FT spectra were collected with a Nicolet 60SX instrument equipped with a standard DRIFTS accessory (± 1 cm^{-1} resolution). The instrument was not calibrated for the number of Lewis and Brønsted acid sites and, consequently, only relative amounts of Lewis and Brønsted acid sites are reported. The relative amount of acid sites is defined as the amount of acid sites in the promoted samples as a fraction of the amount of acid sites in the unpromoted samples.

Temperature-Programmed Reduction

The TPR experiments were performed by initially heating the catalysts to 500°C for 1 h in an O_2/He stream to desorb adsorbed moisture. The samples were then cooled to room temperature and the gas was switched to a 5% H_2/Ar stream. Samples were heated at a rate of 5°C/min, and H_2 consumption was measured with a thermal conductivity detector.

RESULTS

Raman Spectroscopy

The Raman spectra of dehydrated titania-supported vanadia catalysts are shown in Fig. 1, from 700 to 1200 cm^{-1}, as a function of vanadia loading. The TiO_2 support possesses a Raman band at 790 cm^{-1} which diminishes in intensity with increasing vanadia loading due to the absorption of the laser light by the yellow-orange-colored vanadia component. Addition of vanadia to the titania support results in the appearance of two new Raman bands at ~1030 and ~930 cm^{-1} which have previously been assigned to isolated and polymerized surface vanadia species, respectively (3, 24). The sharp Raman band of the isolated surface vanadia species shifts from 1025 to 1030 cm^{-1} as a function of surface vanadia coverage. The ratio of polymerized to isolated surface vanadia species increases with vanadia loading up to monolayer coverage (approximately 6% V_2O_5/TiO_2, which corresponds to 13.2 μmol V^{+5}/m^2). At higher vanadia loadings on titania (8% V_2O_5/TiO_2), microcrystalline V_2O_5 particles are formed as separate phases on the two-dimensional surface vanadia overlayer and give rise to a strong Raman band at 994 cm^{-1} (24). Therefore, two surface vanadia species, isolated and polymerized, as well as a microcrystalline phase, V_2O_5 particles, are present in the titania-supported vanadia catalysts and their relative concentrations depend on the surface vanadia coverage.

The influence of promoters (tungsten oxide, niobium oxide, and sulfate) on the Raman spectrum of a 1% V_2O_5/TiO_2 catalyst under dehydrated conditions is shown in Fig. 2 in the region 700–1200 cm^{-1}. The unpromoted 1% V_2O_5/TiO_2 catalyst exhibits a sharp Raman band at 1025 cm^{-1} which is shifted toward 1030 cm^{-1} on the addition of tungsten and niobium oxide promoters. This slight shift reflects the higher surface coverages brought about by the addition of tungsten and niobium oxides, which are present as surface metal oxide species (see below). The addition of 1.1% SO_4 to the 1% V_2O_5/TiO_2 catalyst results in a downward shift and decrease in relative intensity of the 1025 cm^{-1} Raman band. The total surface coverages of the mixed metal oxide overlayers were maintained below monolayer coverages and are presented in Table 1. Monolayer surface coverage on the titania support for the promoters corresponds to 7% Nb_2O_5/TiO_2 (10.5 μmol Nb^{+5}/m^2) (25) and 8% WO_3/TiO_2 (6.9 μmol W^{+6}/m^2) (24), and only 1.1% SO_4 (2.2 μmol S^{+6}/m^2) is achievable for the surface sulfate because of its volatility.

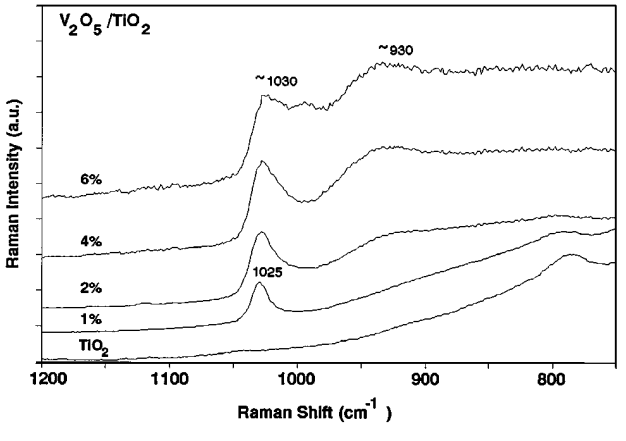

FIG. 1. Raman spectra of V_2O_5/TiO_2 catalysts under dehydrated conditions as a function of vanadia loading.

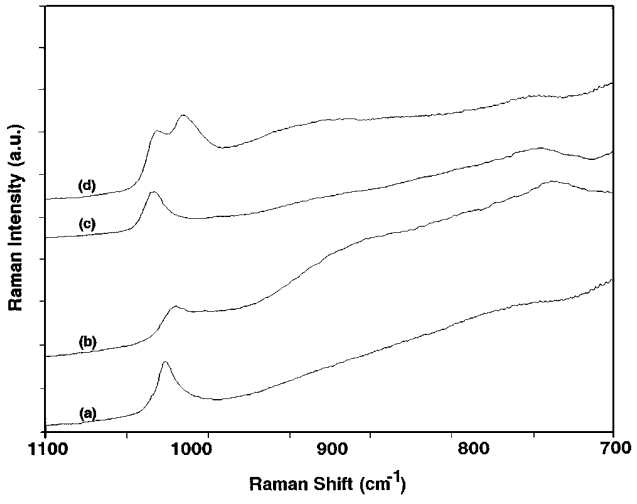

FIG. 2. Raman spectra of promoted 1% V_2O_5/TiO_2 catalysts under dehydrated conditions. (a) 1% V_2O_5/TiO_2, (b) 1.1% SO_4/1% V_2O_5/TiO_2, (c) 6% Nb_2O_5/1% V_2O_5/TiO_2, (d) 7% WO_3/1% V_2O_5/TiO_2.

The tungsten oxide and niobium oxide promoters only mildly influenced the 925–930 cm^{-1} Raman bands associated with the polymerized surface vanadia species. For the 1.1% SO_4/1% V_2O_5/TiO_2 catalyst the increase in intensity of the 925–930 cm^{-1} Raman band is more obvious but not comparable to the increase observed when the vanadium oxide loading is increased (compare Figs. 1 and 2). The promoters only formed surface metal oxide phases since the Raman bands of crystalline WO_3 (24) and Nb_2O_5 (25) phases were absent. The surface tungsten oxide species gave rise to a Raman band at 1011 cm^{-1} (24) (see Fig. 2), and the surface sulfate species exhibited a Raman band at 1370 cm^{-1} (not

TABLE 1

Surface Coverages of Mixed Metal Oxide Catalysts

Catalyst	V (μmol/m^2)	Promoter atom (μmol/m^2)	Total (μmol/m^2)
1% V_2O_5/TiO_2	2.2	—	2.2
7% WO_3/1% V_2O_5/TiO_2	2.2	6.0	8.2
6% Nb_2O_5/1% V_2O_5/TiO_2	2.2	9.0	11.2
1.1% SO_4/1% V_2O_5/TiO_2	2.2	2.3	4.5

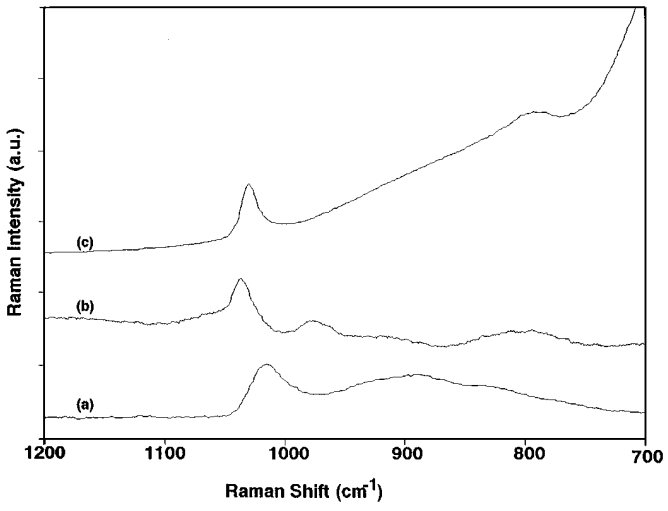

FIG. 3. Raman spectra of 1% V_2O_5 supported on (a) alumina, (b) silica, and (c) titania under dehydrated conditions.

shown in Fig. 2) (21). The surface niobium oxide species possesses Raman bands at 985 and 930 cm^{-1}, but is overshadowed by the much stronger Raman band of the surface vanadia species (25). Thus, the promoters increase the apparent surface coverage of the surface vanadia species and have only a mild (tungsten oxide and niobium oxide) to moderate (sulfate) influence on the ratio of polymerized to isolated surface vanadia species.

The Raman spectra of 1% V_2O_5 supported on different oxides (alumina, titania, and silica) under dehydrated condtions are presented in Fig. 3 in the region 700–1200 cm^{-1}. At these low surface coverages, the isolated surface vanadia species is the predominant vanadia species present on the different oxide supports and gives rise to a sharp Raman band at 1016, 1025, and 1039 cm^{-1} for alumina, titania, and silica, respectively. For the 1% V_2O_5/Al_2O_3 a Raman band at 880 cm^{-1} of lesser relative intensity is also observed, but is a minor component. The 970 and 800 cm^{-1} bands in spectrum b and 790 cm^{-1} band in spectrum c of Fig. 3 arise from the SiO_2 and TiO_2 supports, respectively. The shift in position of the Raman band of the surface vanadia species is due to slight changes, approximately 0.02 Å, in the length of the terminal V=O bond (26) of the surface $O{=}V(-O-S)_3$ species (27, 28), where S represents the oxide support cation (Al, Ti, or Si).

Surface Acidity

The distribution of surface acid sites in the titania-supported vanadia catalysts as a function of vanadia loading has previously been reported in the literature (29). The titania support possesses only weak surface Lewis acid sites and no surface Brønsted acid sites as measured by pyridine adsorption (30). The number of surface Lewis acid sites slightly decreases and the number of surface Brønsted acid sites significantly increases as the surface vanadia loading is increased on the titania support (29).

The effect of promoters on the acidity measured by pyridine adsorption of 1% V_2O_5/TiO_2 depends on the specific promoter used. The influence of the promoters on the acidity of the 1% V_2O_5/TiO_2 catalyst is shown in Table 2. The addition of the surface niobium oxide and sulfate promoters does not have an influence on the surface Brønsted acidity characteristics of the V_2O_5/TiO_2 catalyst, but the Lewis acidity appears to remain unchanged for the surface niobium oxide species and decreases for the surface sulfate species. However, the addition of the surface tungsten oxide promoter to the vanadia–titania catalyst has a dramatic influence on the surface Brønsted acidity of the catalyst. These findings are in agreement with the intrinsic acidities of these promoters on a titania support since Nb_2O_5/TiO_2 does not possess surface Brønsted acidity (30), SO_4/TiO_2 possesses surface Brønsted acidity only at high surface coverages (31), and WO_3/TiO_2 possesses a significant amount of surface Brønsted acidity (especially for the high surface coverages employed in the present investigation) (32).

The acidity of the 1% V_2O_5 supported on different oxides is determined primarily by the acidic characteristics of the oxide support because of the very low surface vanadia coverages. Essentially no surface acid sites were present for the vanadia–silica catalyst, only surface Lewis acid sites were present for the vanadia–alumina catalyst (33), and primarily surface Lewis acid sites with a trace of surface Brønsted acid sites were present for the vanadia–titania catalyst (Table 2).

Therefore, surface Brønsted acidity (measured by pyridine adsorption) is essentially not present at low surface vanadia coverages on oxide supports, but increases with surface vanadia coverage and specific promoters such as surface tungsten oxide species. More recent studies indicate that NH_3 adsorption does give rise to Brønsted acidity for samples that do not show increased Brønsted acidity with pyridine as the base, for example, the $Nb_2O_5/V_2O_5/TiO_2$ catalysts (34). However, pyridine adsorption detects only the stronger Brønsted acid sites because it is a weaker base than NH_3, and pyridine adsorption also readily discriminates between Brønsted and Lewis acid sites than NH_3 adsorption.

TABLE 2

Surface Acidity Characteristics of Promoted 1% V_2O_5/TiO_2 Catalysts

Catalysts	Relative Brønsted acidity (arbitrary units)	Relative Lewis acidity (arbitrary units)
1% V_2O_5/TiO_2	1	1
6% WO_3/1% V_2O_5/TiO_2	2.9	0.3
3% Nb_2O_5/1% V_2O_5/TiO_2	~1	0.9
1.1% SO_4/1% V_2O_5/TiO_2	~1	0.3

Redox Properties

The redox properties of the titania-supported vanadia catalysts were determined as a function of surface vanadia coverage and specific promoters by the selective oxidation of methanol at 503 K. This reaction probe was selected because methanol oxidation to formaldehyde requires only one surface redox site and yields dimethyl ether over surface acid sites (19). The selectivity toward formaldehyde varied from 95 to 99% and the major byproduct was dimethoxymethane, which is also a redox product of methanol oxidation. Only trace quantities of dimethyl ether were produced, indicating that surface acid sites were essentially not participating during the methanol oxidation reaction over the vanadia–titania catalysts. The TOFs for the titania-supported vanadia catalysts are presented in Figs. 4 and 5 as a function of vanadia loading and promoters, respectively. Within experimental error, the methanol oxidation TOF does not appear to depend on the surface vanadia coverage, over the 1–7% V_2O_5 loading, or the presence of the selected promoters (surface tungsten oxide, surface niobium oxide, and surface sulfate). Independent methanol oxidation studies revealed that surface tungsten oxide, surface niobium oxide, and surface sulfate species on titania did not possess redox characteristics since they did not yield any formaldehyde at 503 K for the chosen reaction conditions (20, 21). The 7% V_2O_5/TiO_2 sample contained a small amount of microcrystalline V_2O_5 particles; the overall dispersion or fraction exposed was estimated to be about 90%, which did not significantly affect the apparent TOF. Higher concentrations of crystalline V_2O_5 particles present at a higher vanadia loading do in fact decrease the apparent TOFs of the vanadia–titania catalysts. Thus, the specific redox properties of the titania-supported vanadia catalysts are not a function of the surface vanadia coverage or the presence of the selected promoters (surface tungsten oxide, niobium oxide, and sulfate).

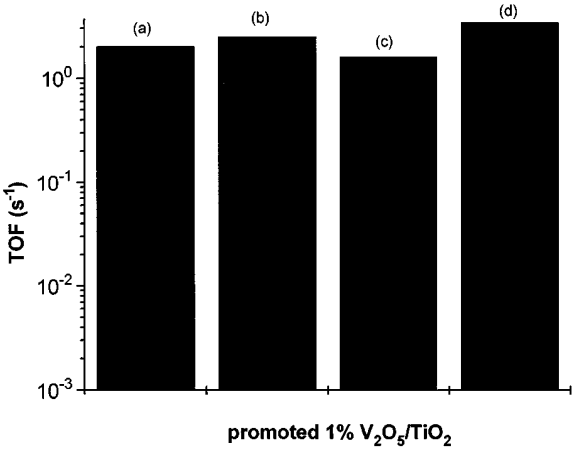

FIG. 5. Redox reactivity of promoted V_2O_5/TiO_2 catalysts during methanol oxidation (503 K). (a) 1% V_2O_5/TiO_2, (b) 1.1% SO_4/1% V_2O_5/TiO_2, (c) 6% Nb_2O_5/1% V_2O_5/TiO_2, (d) 7% WO_3/1% V_2O_5/TiO_2.

The influence of the oxide support on the redox properties of the supported vanadia catalysts was also examined and the methanol oxidation redox TOFs are shown in Fig. 6. The selectivity toward formaldehyde was reduced by the participation of the alumina and silica supports in the methanol oxidation reaction which resulted in the formation of dimethyl ether and dimethyl ether/carbon oxides, respectively. However, the redox TOF only measures the reactivity of the surface vanadia sites toward formaldehyde production and, consequently, neglects the reactivity of the support. The specific oxide support has a dramatic effect on the methanol oxidation redox TOF and varies by approximately three orders of magnitude ($V_2O_5/TiO_2 \gg V_2O_5/Al_2O_3 > V_2O_5/SiO_2$).

The influence of the specific oxide support on the redox properties of the surface vanadia species was also probed with TPR in a hydrogen/helium mixture. The reduction

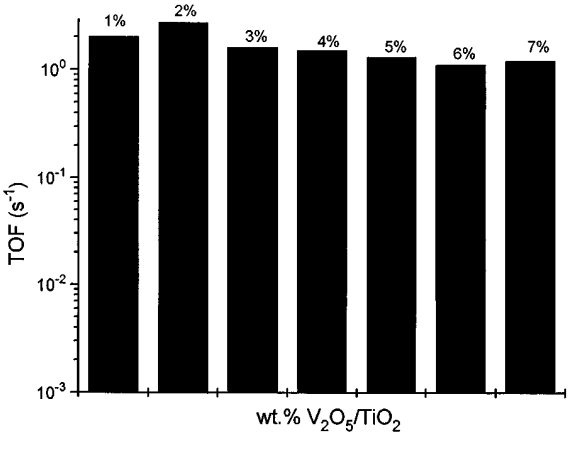

FIG. 4. Redox reactivity of V_2O_5/TiO_2 catalysts during methanol oxidation as a function of V_2O_5 loading (503 K).

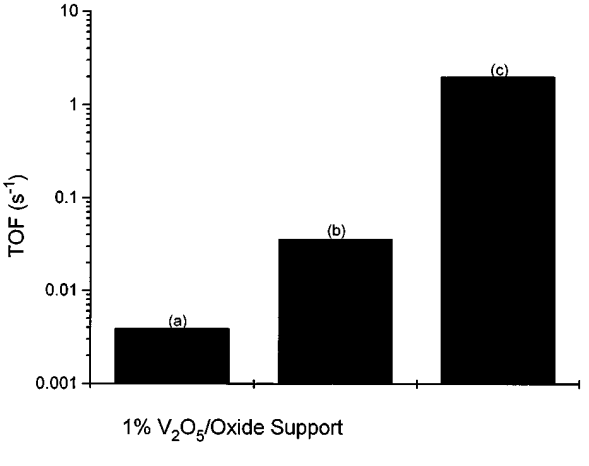

FIG. 6. Redox reactivity of 1% V_2O_5 supported on (a) SiO_2, (b) Al_2O_3, and (c) TiO_2 during methanol oxidation (503 K).

TABLE 3

TPR Peak Maxima for 1% V_2O_5 Supported on Different Oxides

Catalyst	T_p (K)
1% V_2O_5/TiO_2	654
1% V_2O_5/Al_2O_3	714
1% V_2O_5/SiO_2	721

peak maxima during TPR for the different supported vanadia catalysts are presented in Table 3. The differences in the TPR results are not as dramatic as the methanol oxidation TOFs, but exhibit the same trend ($V_2O_5/TiO_2 > V_2O_5/Al_2O_3 > V_2O_5/SiO_2$). The TPR results confirm that the specific oxide support does have an effect on the redox properties of the surface vanadia species.

DeNOx Properties

The TOFs for the selective catalytic reduction of NO with NH_3 over titania-supported vanadia catalysts as a function of vanadia loading are shown in Fig. 7. The selectivity toward N_2 production is essentially 100% for this series of catalysts at 473 K and chosen experimental conditions. The SCR TOF increases with increasing vanadia content by a factor of 5 up to monolayer surface coverage, 6% V_2O_5/TiO_2, and decreases above monolayer coverage where microcrystalline V_2O_5 particles are present. The 40% decrease in the SCR TOF above monolayer coverage is significantly greater than the corresponding decrease in the dispersion of the vanadia species (from 100% at monolayer coverage to approximately 80% for the 8% V_2O_5/TiO_2 catalyst). This suggests that the microcrystalline V_2O_5 particles are less reactive than the surface vanadia species as well as interfere with the reactivity of the surface vanadia species during the SCR reaction.

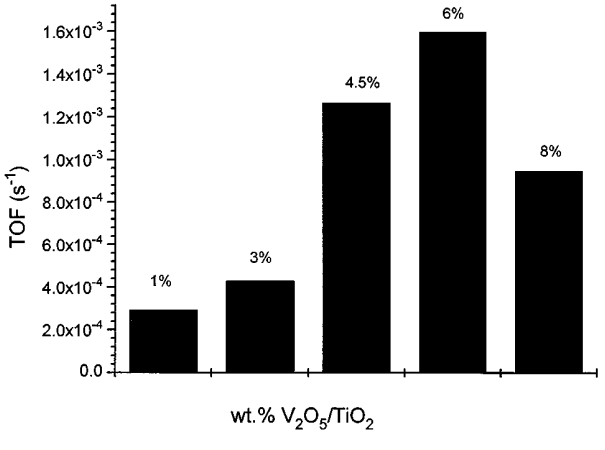

FIG. 7. SCR reactivity of V_2O_5/TiO_2 catalysts as a function of V_2O_5 loading (473 K).

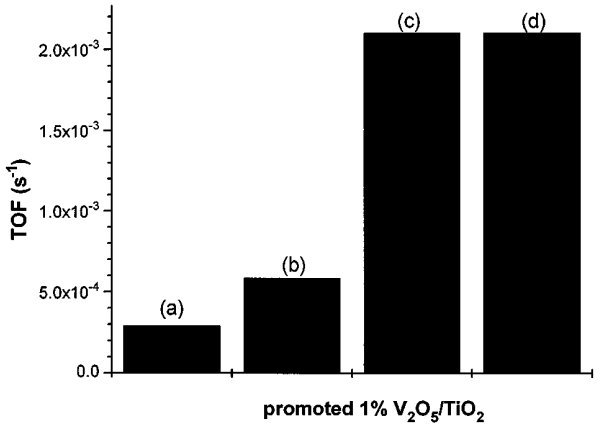

FIG. 8. SCR reactivity of promoted 1% V_2O_5/TiO_2 catalysts (473 K). (a) 1% V_2O_5/TiO_2, (b) 1.1% SO_4/1% V_2O_5/TiO_2, (c) 6% Nb_2O_5/1% V_2O_5/TiO_2, (d) 7% WO_3/1% V_2O_5/TiO_2.

The influence of the promoters on the SCR TOF is presented in Fig. 8. The selectivity toward N_2 production is essentially 100% for this series of catalysts at 473 K under the chosen reaction conditions. The introduction of the surface sulfate species increased the SCR TOF by a factor of 2, and the introduction of surface tungsten oxide and niobium oxide species increased the SCR TOF by approximately an order of magnitude. Consequently, the specific SCR reactivity of the titania-supported vanadia catalysts is dependent on the surface vanadia coverage and the presence of the selected promoters (surface tungsten oxide, niobium oxide, and sulfate species).

The selectivity of SCR DeNOx catalysts at 100% NO conversion is also an important parameter. All the titania-supported vanadia SCR catalysts achieved 100% NO conversion at 623 K. The SCR selectivities toward N_2 formation at 100% NO conversion are listed in Table 4 as a function of vanadium oxide loading and promoters. Increasing the vanadium oxide loading beyond 3% results in a drop in N_2 selectivity from 100 to 73%. Furthermore, the addition of tungsten oxide and sulfate decrease the selectivity to N_2 formation, 91 and 94%, respectively, whereas the addition of niobium oxide maintains the selectivity to N_2 at 100%.

TABLE 4

SCR Selectivities at 100% NO Conversion (623 K)

Catalyst	N_2 selectivity (%)
1% V_2O_5/TiO_2	100
3% V_2O_5/TiO_2	100
4.5% V_2O_5/TiO_2	85
6% V_2O_5/TiO_2	78
8% V_2O_5/TiO_2	73
6% Nb_2O_5/1% V_2O_5/TiO_2	100
7% WO_3/1% V_2O_5/TiO_2	91
1.1% SO_4/1% V_2O_5/TiO_2	94

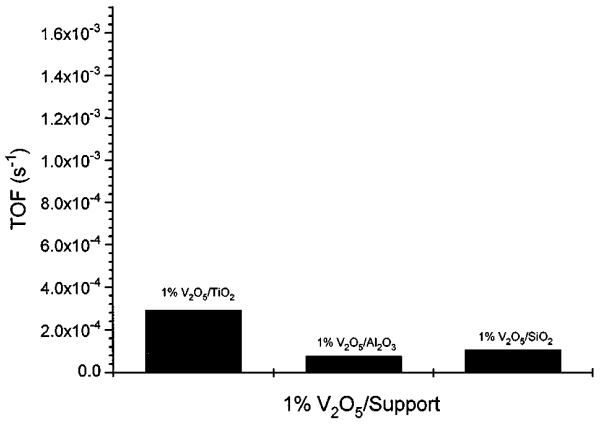

FIG. 9. SCR reactivity of 1% V_2O_5 supported vanadia catalysts on different oxide supports (473 K). Note: same scale as in Fig. 7.

Therefore, at 100% conversion of NO, increasing the surface vanadia coverage lowers the selectivity toward N_2 due to formation of N_2O and the specific promoters can further modify the selectivity.

The TOFs for the SCR of NO with NH_3 over 1% V_2O_5 on different oxides are presented in Fig. 9. The oxide supports, in the absence of vanadia, exhibited negligible conversion during the SCR reaction. The TOF for the vanadia–titania catalyst was approximately three times greater than those for the vanadia–alumina and vanadia–silica catalysts. This trend was also observed for the alumina and titania systems at monolayer coverage of surface vanadia (factor of 4). Monolayer surface coverage of vanadia on silica is not achievable (28) and, consequently, could not be measured. The SCR selectivities of the different 1% V_2O_5 catalysts are presented in Table 5. The SCR selectivity of 1% V_2O_5/TiO_2 is found to be better than 1% V_2O_5/Al_2O_3 and 1% V_2O_5/SiO_2 at 473 and 623 K. The selectivity to N_2 of 1% V_2O_5/Al_2O_3 and 1% V_2O_5/SiO_2 decreases further at 623 K but remains 100% for 1% V_2O_5/TiO_2. Thus, the oxide support affects both the specific reactivity and selectivity of the selective catalytic reduction of NO with NH_3 over supported vanadia catalysts.

In Situ Raman Spectroscopy during DeNOx

In situ Raman experiments during the SCR reaction were also undertaken to monitor the stability of the terminal

TABLE 5

SCR Selectivities for 1% V_2O_5 on Different Oxide Supports

	N_2 selectivity (%)	
Catalyst	473 K	623 K
1% V_2O_5/TiO_2	100	100
1% V_2O_5/Al_2O_3	94	91
1% V_2O_5/SiO_2	91	85

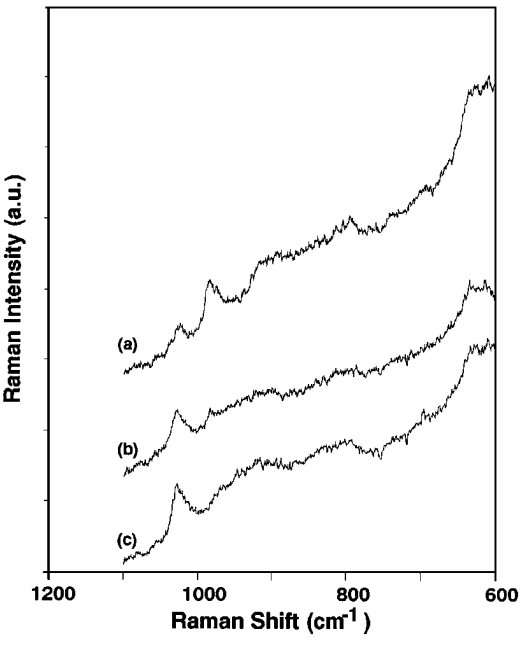

FIG. 10. *In situ* Raman spectra of 4% V_2O_5/ZrO_2 during SCR reaction at 300°C. (a) After 25 reduction–reoxidation cycles with butane and $^{18}O_2$, respectively and cool down to 300°C. (b) After selective catalytic reduction of NO with NH_3 for 1400 s. (c) After selective catalytic reduction of NO with NH_3 for 1800 s.

V=O bond during this reaction. The terminal bond was isotopically labeled with oxygen-18 via a series of successive butane reduction and ^{18}O oxidation cycles. The heavier mass of oxygen-18 relative to oxygen-16 shifted the corresponding Raman band from approximately 1030 to 990 cm^{-1} (see Fig. 10). The surface vanadia monolayer coverage was deposited on a zirconia support (Degussa, 39 m^2/g) because preliminary experiments revealed that oxygen diffuses less readily through zirconia than titania, and, consequently, the zirconia support minimized the consumption of the expensive oxygen-18. The time required to exchange the terminal $V=^{18}O$ bond to $V=^{16}O$ during the SCR reaction (containing only $^{16}O_2$ and NO) was monitored by Raman spectroscopy (see Fig. 10). This exchange process took approximately 1800 s to complete. Comparison of the exchange time, $t_{ex} = 1800$ s, with characteristic reaction time, $t_{rx} = 1/\text{TOF} = 182$ s, reveals that it took approximately 10 reaction cycles to completely exchange the isotopically labeled $V=^{18}O$ terminal bond. This novel experiment suggests that the terminal V=O bond is too stable during the SCR reaction to be directly involved in the rate-determining step.

DISCUSSION

Increasing the surface vanadia coverage up to monolayer coverage increased the density (active sites/m^2) of surface redox sites, the ratio of polymerized to isolated

surface vanadia species, the number of surface Brønsted acid sites, and the SCR DeNOx TOF, but did not affect the specific redox properties of the surface vanadia species. The constant methanol oxidation TOF, the redox probe reaction, with surface vanadia coverage reflects the one redox site requirement of this unimolecular reaction (19, 35) and the constant specific redox potential of the surface vanadia species at all coverages. The increasing SCR TOF with surface vanadia coverage reflects that the bimolecular DeNOx reaction requires another site in addition to the redox site to proceed. This requirement of an additional surface site suggests that the immediate environment of the surface redox site is critical. The increase in the SCR TOF with surface vanadia coverage could originate from the need for the DeNOx reaction to have two adjacent surface redox sites, a surface redox site with an adjacent surface acid site, or the greater specific activity of polymerized surface vanadia species relative to the isolated surface vanadia species. However, it is not straightforward to discriminate among these different possibilities by varying the surface vanadia coverage on titania since all of the above scenarios increase monotonically with surface vanadia coverage.

The introduction of surface promoters to the titania supported vanadia catalyst system introduces an independent variable which provides additional fundamental insight into the SCR DeNOx reaction and allows for better discrimination among the above possible scenarios. The addition of surface tungsten oxide, niobium oxide, and sulfate species to the 1% V_2O_5/TiO_2 catalyst increased the SCR TOF up to an order of magnitude at 473 K, with the maximum TOF observed for the tungsten oxide- and niobium oxide-promoted catalyst. The methanol oxidation probe reaction studies revealed that none of these surface promoter species were redox sites under these reaction conditions and infrared studies showed that the tungsten oxide promoter was a surface Brønsted acid site. The niobium oxide and sulfate promoters did not appear to substantially change the acidity of the 1% V_2O_5/TiO_2 catalyst. These observations suggest that the addition of surface non-reducible metal oxide sites to surface redox sites substantially enhances the SCR TOF of titania-supported vanadia catalysts. It also demonstrates that the DeNOx reaction does not necessarily require two adjacent surface redox sites to proceed. Examination of the Raman spectra in Fig. 2 and the SCR data in Fig. 8 shows that the introduction of the surface promoter species has only a minor effect on the ratio of polymerized to isolated surface vanadia species but an enhancement of the SCR TOF is observed. Thus, it appears that the DeNOx reaction occurs most efficiently over a pair of surface sites containing a surface redox site and an adjacent surface nonreducible metal oxide site.

The different enhancements of the surface promoters on the DeNOx reaction over the 1% V_2O_5/TiO_2 catalyst are due to their different surface concentrations and acidic properties. Only a factor of 2 increase in the SCR TOF was obtained when the surface sulfate promoter was added. For the sulfated sample additional sulfate could not be added because it is not possible to achieve a high surface coverage of this surface species due to its volatility (see Table 1). The addition of surface niobium oxide and tungsten oxide species resulted in almost an order of magnitude increase in the SCR TOFs because of the high surface coverages of these promoters (see Table 1). The relative influence of the promoters, per promoter atom, on the SCR reaction are $W \cong 1.7$, $Nb \cong 1.1$, and $S \cong 0.9$. The surface tungsten oxide species possessed Brønsted acid sites, and the increase in the SCR TOF reveals the promoting effect of such sites. Comparison of the SCR TOF enhancements by the surface niobium oxide and tungsten oxide promoters suggests that surface Brønsted acid sites are the most efficient in promoting the SCR reaction since fewer surface tungsten oxide species resulted in a comparable TOF. Topsoe *et al.* recently provided *in situ* spectroscopic evidence that both surface Brønsted acid sites, and surface V=O sites are involved in the SCR catalytic cycle over vanadia–titania catalysts (14, 15). However, it should be noted that the presence of Brønsted acidity (as measured by pyridine adsorption) is not entirely necessary for the enhancement of the SCR reaction (e.g., niobium oxide).

The active surface sites for the SCR DeNOx reaction are also influenced by the underlying oxide support, and the TOFs vary by a factor of approximately 3 at 473 K and the chosen experimental conditions. The redox properties of the surface vanadia species are influenced by the underlying oxide support as shown by the very sensitive methanol oxidation reaction and TPR measurements: surface vanadia reduces more readily on $TiO_2 \gg Al_2O_3 > SiO_2$. The acidic properties of the surface vanadia species are slightly influenced by the oxide support since 1% V_2O_5 on titania possesses a small amount of surface Brønsted acid sites and surface Brønsted acid sites are not present on the corresponding 1% V_2O_5 on alumina and silica supports. However, comparable numbers of surface redox and Brønsted acid sites (per square meter) are present at monolayer coverages for alumina- and titania-supported vanadia catalysts (29, 33) and the difference in TOF is still present. This suggests that the specific redox properties of the surface vanadia species are primarily responsible for the influence of the oxide support on the SCR TOF. Furthermore, the specific oxide support also has an influence on the selectivity toward N_2 formation ($TiO_2 > Al_2O_3 > SiO_2$) as shown in Table 5 which may also be related to specific redox properties of the surface vanadia species. Similar observations about the influence of the oxide support on the SCR reactivity of the surface vanadia species were also reported by Nickl *et al.* (36).

Comparison of the SCR TOFs with the terminal V=O bond lengths or strengths, as directly measured by Raman

spectroscopy (26), also reveals that a correlation between these two parameters does not appear to exist. The most active vanadia–titania catalyst exhibited a V=O Raman band 1025 cm^{-1}, while the less active vanadia–alumina and vanadia–silica catalysts exhibited V=O Raman bands at 1016 and 1037 cm^{-1}, respectively. The terminal V=O bond is clearly perturbed by the reduction as well as adsorption of hydrogen-containing gases such as NH_3 (4, 14, 15) and H_2O (24, 28) due to hydrogen bonding, but these observations do not prove that it is directly involved in the rate-determining step during the DeNOx reaction. The influence of the oxide support on the surface vanadia redox properties and the SCR TOF suggests that the bridging V–O–support bond may contribute to the rate determining step of the DeNOx reaction. This conclusion is consistent with model SCR studies with unsupported V_2O_5 crystals that reported that the crystallographic planes possessing V–O–V or V–OH bonds rather than V=O bonds were the selective sites for the SCR reaction (12, 13). The *in situ* Raman experiments during the SCR reaction further support the above conclusion since V=^{18}O was formed to be relatively stable during the SCR reaction ($t_{ex}/t_{rx} \sim 10$).

The most efficient catalyst for the DeNOx reaction appears to be the titania-supported vanadia catalyst since it yields the highest TOF and selectivity in comparison to the corresponding alumina and silica catalyst systems. The selectivity toward N_2 is 100% for the vanadia–titania system, and is not affected by the crystalline V_2O_5 or promoters at 473 K. However, at 623 K the selectivities deviated from 100% N_2 production with surface vanadia coverage and the introduction of promoters (see Table 4). The selectivity toward N_2 remained 100% up to 0.5 monolayer coverage and decreased with increasing surface vanadia coverage up to monolayer coverage. This suggests that a high surface concentration of surface vanadia redox sites, especially pairs of surface vanadia sites, may lead to overoxidation of NH_3 and NO to N_2O during the DeNOx reaction at elevated temperatures. The introduction of surface sulfate to the 1% V_2O_5/TiO_2 catalyst decreased the N_2 selectivity from 100 to 94%. Additional DeNOx studies with sulfated titania, in the absence of surface vanadia, demonstrated that the surface sulfate species becomes active as a redox site at 623 K, and results in 50% conversion of NO and a 93% selectivity to N_2 for comparable amounts of catalysts. Similarly, the surface tungsten oxide species on titania also becomes active as a redox site at elevated temperatures (37). The surface niobium oxide species on titania is very stable to reduction by ammonia (38). An 8.8% Nb_2O_5/TiO_2 catalyst resulted in 42% conversion of NO and an N_2 selectivity of 83% at 623 K (39), but this catalyst had more than a monolayer of surface niobium oxide species, which corresponds to 7% Nb_2O_5/TiO_2. The 100% N_2 selectivity for the niobium oxide-promoted 1% V_2O_5/TiO_2 catalyst suggests that the surface niobium oxide species are not significantly participating as redox sites in the DeNOx reaction at 623 K since lower selectivities would be expected. At elevated temperatures, high concentrations of surface redox sites, or pairs of surface redox sites, appear to result in overoxidation of NH_3 and NO to N_2O and lower the DeNOx selectivity.

In summary, the data presented above suggest that selective catalytic reduction of NO_x with NH_3 proceeds most efficiently over a dual-site mechanism involving a surface vanadia redox site and an adjacent surface nonreducible metal oxide site. The SCR reaction appears to be faster when the surface acid site is a Brønsted acid site; it can also proceed with a surface nonreducible metal oxide site, but the efficiency of the DeNOx reaction is usually reduced. When the adjacent surface site behaves as a redox site, the selectivity to N_2 may be reduced by ammonia oxidation to N_2O at elevated temperatures. The above dual-site mechanism for the SCR reaction has many features in common with prior mechanisms proposed in the literature. The need for two sites for the DeNOx reaction has also been proposed by Miyamoto *et al.* (1) (ammonia is adsorbed as NH_4^+ adjacent to V=O sites) and Janssen *et al.* (2) (pyrovanadate structure, O=V–O–V=O, is the most likely active site). The adsorption of NH_3 primarily on surface Lewis acid sites was proposed by Lietti *et al.* (6, 7) and Went *et al.* (4). More recently, Topsoe *et al.* provided convincing *in situ* spectroscopic evidence that both surface Brønsted acid sites and surface vanadia sites are involved in the SCR catalytic cycle over titania-supported vanadia catalysts (14, 15). The conclusions reached above may have to be slightly modified when extrapolating to the more severe industrial DeNOx conditions where higher temperatures, significant amounts of moisture, sulfur oxides, and poisons are encountered.

CONCLUSIONS

The structure and reactivity of supported vanadia catalysts were investigated as a function of surface coverage, promoters, specific oxide support, and temperature. The molecular structures of the surface vanadia species were determined with Raman spectroscopy and the distribution of surface Brønsted and Lewis acid sites was measured by infrared spectroscopy employing pyridine adsorption. The redox potential of the surface vanadia species was monitored by methanol oxidation and TPR. The reactivity of the various catalysts for the selective catalytic reduction of NO_x with NH_3 was measured over a wide temperature range. Comparison of the structure and reactivity properties of the supported vanadia catalysts suggests that the reaction proceeds via a dual-site mechanism, involving a surface vanadia redox site and an adjacent surface nonreducible metal oxide site. Such dual sites are generated with increasing surface coverage of surface vanadia species or the addition of promoters, such as surface oxides of tungsten, niobium, and sulfur, and result in a 5- to 10-fold increase in the SCR TOF.

The specific oxide support also influences the redox properties of the surface vanadia species, which can affect the SCR TOF by a factor of approximately 3 as well as the selectivity toward N_2 production. This observation along with the stability of the terminal $V{=}^{18}O$ bonds during the SCR reaction suggests that the bridging V–O–support bond is involved in the rate-determining step. At elevated temperatures, the selectivity to N_2 may be compromised by ammonia oxidation to N_2O when a high concentration of surface redox sites, especially pairs of surface redox sites, is present. The fundamental insights generated from this investigation have resulted in a better understanding of the nature of the active sites involved in the selective catalytic reduction of NO_x with NH_3.

ACKNOWLEDGMENT

The financial assistance of DOE (Office of Basic Energy Sciences) Grant DE-FG02-93ER14350 is gratefully acknowledged by G.D. and I.E.W.

REFERENCES

1. Miyamoto, A., Yamazaki, Y., Inomata, M., and Murakami, Y., *J. Phys. Chem.* **85**, 2366 (1981).
2. Janssen, F. J. J. G., van den Kerkhof, F. M. G., Bosch, H., and Ross., J. R. H., (a) *J. Phys. Chem.* **1**, 5921 (1987); (b) *J. Phys. Chem.* **91**, 6683 (1987).
3. Went, G. T., Leu, L.-J., and Bell, A. T., *J. Catal.* **134**, 479 (1992).
4. Went, G. T., Leu, L.-J., Rosin, R. R., and Bell, A. T., *J. Catal.* **134**, 492 (1992).
5. Handy, B. E., Maciejewski, M., and Baiker, A., *J. Catal.* **134**, 75 (1992).
6. Lietti, L., Svachula, J., Forzatti, P., Busca, G., Ramis, G., and Bregani, F., *Catal. Today* **17**, 131 (1993).
7. Ramis, G., Busca, G., Bregani F., and Forzatti, P., *Appl. Catal.* **64**, 259 (1990).
8. Ramis, G., Busca, G., and Bregani, F., *Catal. Lett.* **18**, 299 (1993).
9. Topsoe, N.-Y., *J. Catal.* **128**, 499 (1991).
10. Rajadhyaksha, R. A., and Knozinger, H., *Appl. Catal.* **51**, 81 (1989).
11. Chen, J. P., and Yang, R. T., *J. Catal.* **125**, 411 (1990).
12. Gasior, M., Haber, J., Machej, T., and Czeppe, T., *J. Mol. Catal.* **43**, 359 (1988).
13. Ozkan, U. S., Cai, Y., and Kumthekar, M., *Appl. Catal. A* **96**, 365 (1993).
14. Topsoe, N.-Y., Topsoe, H., and Dumesic, J. A., *J. Catal.* **151**, 226 (1995).
15. Topsoe, N.-Y., Dumesic, J. A., and Topsoe, H., *J. Catal.* **151**, 241 (1995).
16. Odriozola, J. A., Heinemann, H., Somorjai, G. A., Garcia de la Banda, J. F., and Pereira, P., *J. Catal.* **119**, 71 (1989).
17. Takagi, M., Kawai, T., Soma, M., Onishi, T., and Tamaru, K., *J. Catal.* **57**, 528 (1979).
18. Dumesic, J. A., Topsoe, N.-Y., Slabiak, T., Morsing, P., Clausen, B. S., Tornqvist, E., and Toposoe, H., *in* "Proceedings, 10th International Congress on Catalysis, Budapest, 1992" (L. Guczi, F. Solymosi, and P. Tetenyi, Eds.), p. 1325. Akadémiai Kiadó, Budapest, 1993.
19. Deo, G., and Wachs, I. E., *J. Catal.* **146**, 323 (1994).
20. Deo, G., and Wachs, I. E., *J. Catal.* **146**, 335 (1994).
21. Jehng, J. M., and Wachs, I. E., to be published.
22. Jehng, J.-M., Deo, G., and Wachs, I. E., *J. Mol. Catal.*, in press.
23. Andreini, A., de Boer, M., Vuurman, M. A., Deo, G., and Wachs, I. E., *J. Chem. Soc., Faraday Trans.*
24. Vuurman, M. A., Wachs, I. E., and Hirt, A. M., *J. Phys. Chem.* **95**, 9928 (1991).
25. Jehng, J. M., and Wachs, I. E., *J. Phys. Chem.* **95**, 7373 (1991).
26. Hardcastle, F. D., and Wachs, I. E., *J. Phys. Chem.* **95**, 5031 (1991).
27. Eckert, H., and Wachs, I. E., *J. Phys. Chem.* **93**, 6796 (1989).
28. Das, N., Eckert, H., Hu, H., Wachs, I. E., Walzer, J. F., and Feher, F. J., *J. Phys. Chem.* **97**, 8240 (1993).
29. Miyata, H., Fujii, K., and Ono, T., *J. Chem. Soc. Faraday Trans. 1* **84**, 3121 (1988).
30. Datka, J., Turek, A. M., Jehng, J. M., and Wachs, I. E., *J. Catal.* **135**, 186 (1992).
31. Waqif, M., Bachelier, J., Saur, O., and Lavalley, J-C., *J. Mol. Catal.* **72**, 127 (1992).
32. Yamaguchi, T., Tanaka, Y., and Tanabe, K., *J. Catal.* **65**, 442 (1980).
33. Turek, A. M., Wachs, I. E., and DeCanio, E., *J. Phys. Chem.* **96**, 5000 (1992).
34. Vikulov, K. V., and Andreini, A., unpublished results.
35. Weber, R. S., *J. Phys. Chem.* **98**, 2999 (1994).
36. Nickl, J., Dutroit, D., Baiker, A., Scharf, U., and Wokaun, A., *Ber. Bunsenges. Phys. Chem.* **97**, 217 (1993).
37. Hilbrig, F., Schmelz, H., and Knözinger, H., *in New Frontiers in Catalysis,* "Proceedings, 10th International Congress on Catalysis, Budapest, 1992" (L. Guczi, F. Solymosi, and P. Tetenyi, Eds.), p. 1351. Akadémiai Kiadó, Budapest, 1993.
38. Pittman, R. M., and Bell, A. T., *Catal. Lett.* **24**, 1 (1994).
39. Vikulov, K. V., Andreini, A., Poels, E. K., and Bliek, A., *Catal. Lett.* **25**, 49 (1994).